Inter-Numerology Interference Pre-Equalization for 5G Mixed-Numerology Communications

2022 IEEE 95th Vehicular Technology Conference (VTC2022-Spring) | 978-1-6654-8243-1/22/$31.00 ©2022 IEEE | DOI: 10.1109/VTC2022-Spring54318.2022.9860604

Buğra Alp Çevikgibi*, Ali Murat Demirtaş*, Tolga Girici*, and Hüseyin Arslan†‡
*Department of Electrical and Electronics Engineering, TOBB University of Economics and Technology, Ankara, 06560, Turkey
†Department of Electrical and Electronics Engineering, Istanbul Medipol University, Istanbul, 34810, Turkey
‡Department of Electrical and Electronics Engineering, University of South Florida, Tampa, FL, 33620, USA
Email: bugra.cevikgibi@gmail.com, ademirtas@etu.edu.tr, tgirici@etu.edu.tr, huseyinarslan@medipol.edu.tr

***Abstract*—This article proposes a pre-equalization method to remove inter-numerology interference (INI) that occurs in multi-numerology OFDM frame structures of fifth-generation New Radio (5G-NR) and beyond, on the transmitter side. In the literature, guard bands, filters, and interference cancellation methods are used to reduce the INI. In this work, we mathematically model how the INI is generated and show how it can be removed completely for multi-numerology systems by deploying a pre-equalization matrix on the transmitter side. With this pre-equalization method, the need for guard bands and filters is eliminated and spectral efficiency is improved.**

***Index Terms*—5G NR, Inter-Numerology Interference, Mixed Numerology, OFDM**

I. Introduction

FIFTH generation (5G) wireless communication networks will require more flexible resource distribution to support a variety of communication requirements. The use-cases of 5G Networks have been categorized into three main service groups: enhanced mobile broadband (eMBB), massive machine-type communication (mMTC), and ultra-reliable and low latency communication (URRLC) [1]. eMBB provides stable and high throughput to cellular users, mMTC supports a massive number of Internet of Things (IoT) devices with low rate and complexity, and URLLC supports low-latency transmissions of small payloads with very high reliability [1].

In the 5G physical layer, *flexible numerology* is a key enabler of supporting diverse use cases. *Flexible numerology* is obtained by adjusting the subcarrier spacing (SCS) in Orthogonal Frequency Division Multiplexing (OFDM). SCS directly determines the OFDM symbol duration and the Cyclic Prefix (CP). It is closely related to the frequency selectivity of the fading channel and the channel coherence time. Therefore, for different use cases (i.e. channel types, delay requirements, etc.), different numerologies can be suitable. While 4G systems support only one type of numerology with SCS of 15 kHz, 5G supports multiple and flexible numerologies to satisfy diverse requirements of a flexible radio access technology [2].

Multiplexing different numerologies (i.e OFDM with different SCS) adjacently in the frequency domain cause in-band interference. This in-band interference is called inter-numerology interference (INI) and it is caused by the out-of-band emissions which are emitted by OFDM symbols of different numerologies.

Inserting a guard band between adjacent numerologies on the same frequency band is a conventional way to reduce the INI [3]. However, inserting a guard band reduces the spectral efficiency of the system. Scheduling the time and frequency is also used to control INI and minimize the effect of INI [3]. The interference between the numerologies depends on the transmitted numerologies' powers and subcarrier spacings. The works in [4], [5], [6] analyze the INI that occurred between adjacent numerologies. In these studies, it is shown that INI is created on the transmitter side before transmission. In the paper, [7], characteristics of the INI are exploited in order to insert subcarriers in some parts of the guard band. In [5], an iterative interference cancellation algorithm is proposed on the receiver side. However, such methods on the receiver side are disadvantageous due to increased complexity at the mobile receivers.

In this work, we analyze the INI by using discrete Fourier transform equations in the frequency and time domains. Then, we model the INI on each transmitted subcarrier (i.e transmitted symbols) as weighted linear combinations of neighbor numerology's transmitted subcarriers. These weighted linear combinations are expressed as the INI weight matrix. Our contribution is to eliminate the INI by multiplying the inverse of the INI weight matrix (W) as a pre-equalizer at the transmitter side.

Simulation results reveal that INI is completely removed in transmitted subcarriers and theoretical minimum bit error rates (BER) for various modulations on a Rayleigh fading channel are achieved without using any guard band.

The rest of the paper is prepared as follows. In Section II, the classical multi-numerology OFDM is revisited. In Section III, the INI is analyzed by DFT and IDFT matrices, and INI on the numerologies is mathematically modeled. At the end of Section III, INI pre-equalization matrix is derived and illustrated. Section IV presents the simulation results of the proposed INI pre-equalizer. Finally, some concluding remarks and future works are provided in Section V.

II. System Model

We consider a downlink (DL) multi-numerology OFDM system. The standardized numerologies (subcarrier spacings)

978-1-6654-8243-1/22/$31.00 ©2022 IEEE

Authorized licensed use limited to: Istanbul Medipol Universitesi. Downloaded on November 07,2022 at 06:26:24 UTC from IEEE Xplore. Restrictions apply.

for 5G NR are [8]

$$\Delta f^{\mu} = 2^{\mu} \times 15\text{kHz}, \quad \mu = 0, 1, 2, 3, 4. \tag{1}$$

The parameter Δf^{μ} is the subcarrier spacing of numerology μ. Among these numerologies, $\mu = 0, 1, 2$ are allowed in the Frequency Range 1 (FR1), which is below 6 GHz [8]. The transmission spectrum is divided into two equal sub-bands, where each sub-band is assigned to one type of numerology. Assume two different numerologies, $\mu = 0, 1$ are multiplexed onto an OFDM frequency band In the literature usually numerologies 0 and 1 are assumed. The same analysis can be easily carried out for numerology pairs $\mu = 0-2$ or $1-2$ or more than two different numerologies on the same frequency band. Without using any guard band, both numerologies can be generated as

$$X_0(k) = \sum_{k'=0}^{N-1} X_0(k')\delta(k-k'),\; X_0(k) = 0 \,\text{for}\, \frac{N}{2} \leq k \leq N-1 \tag{2}$$

$$X_{1,q}(l) = \sum_{l'=0}^{M-1} X_{1,q}(l')\delta(l-l'),\; X_{1,q}(l) = 0 \,\text{for}\, 0 \leq l \leq \frac{M}{2}-1 \tag{3}$$

where N and M are the discrete Fourier transform and inverse discrete Fourier transform (DFT/IDFT) sizes of the numerologies. Complex modulation symbols are denoted as X_0 and $X_{1,q}$. $N = Q \times M$, where $Q = 2$, $q = 0, 1$ and $\delta(.)$ is the delta function. Index $q = 0, 1$ denotes time-multiplexed symbols of the numerology with wider subchannels (i.e. narrower symbol duration). After subcarrier allocation into sub-bands, CP-added discrete-time OFDM symbols for both numerologies can be generated by the IDFT operation.

$$y_0(n) = \frac{1}{N}\sum_{k=0}^{N-1} X_0(k) e^{\frac{j2\pi k \langle n-N_{cp}\rangle_N}{N}}, \quad 0 \leq n \leq N + N_{cp} - 1 \tag{4}$$

$$y_{1,q}(m) = \frac{1}{M}\sum_{l=0}^{M-1} X_{1,q}(l) e^{\frac{j2\pi l \langle m-M_{cp}\rangle_M}{M}}, \quad 0 \leq m \leq M + M_{cp} - 1 \tag{5}$$

where N_{cp} and M_{cp} are CP duration of both numerologies and $N_{cp} = Q \times M_{cp}$. We denote modulo-N operation as $\langle.\rangle_N$. To create the composite numerology OFDM signal, we must concatenate OFDM symbols $y_{1,q}(m)$ in the discrete-time domain.

$$y_1(n) = \sum_{m=0}^{M+M_{cp}-1} \sum_{q=0}^{Q-1} y_{1,q}(m)\delta(n - m - q(M + M_{cp})) \tag{6}$$

Composite numerology OFDM signal is generated as,

$$y_{composite}(n) = y_0(n) + y_1(n) \tag{7}$$

III. Analysis of INI By DFT and IDFT Matrices

N_{cp}-point CP-added N-point IDFT equation (4) can be written in a matrix form in equation (8) where $\bar{\omega}_0^{kn} = (e^{j2\pi/N})^{kn}$, is the complex conjugate of ω_0^{kn}.

M_{cp}-point CP-added M-point IDFT equation (5) can be written in a matrix form as in equation (9), where $\bar{\omega}_1^{lm} = (e^{j2\pi/M})^{lm}$, is the complex conjugate of ω_1^{lm}.

N-point DFT Matrix for numerology 0 can be written as

$$\begin{bmatrix} X_0(0) \\ X_0(1) \\ \vdots \\ X_0(N-1) \end{bmatrix} = \begin{bmatrix} 1 & 1 & \cdots & 1 \\ 1 & \omega_0 & \cdots & \omega_0^{(N-1)} \\ \vdots & \vdots & \ddots & \vdots \\ 1 & \omega_0^{(N-1)} & \cdots & \omega_0^{(N-1)(N-1)} \end{bmatrix} \begin{bmatrix} y_0(0) \\ y_0(1) \\ \vdots \\ y_0(N-1) \end{bmatrix} \tag{10}$$

M-point DFT Matrix for numerology 1 can be written as

$$\begin{bmatrix} X_1(0) \\ X_1(1) \\ \vdots \\ X_1(M-1) \end{bmatrix} = \begin{bmatrix} 1 & 1 & \cdots & 1 \\ 1 & \omega_1 & \cdots & \omega_1^{(M-1)} \\ \vdots & \vdots & \ddots & \vdots \\ 1 & \omega_1^{(M-1)} & \cdots & \omega_1^{(M-1)(M-1)} \end{bmatrix} \begin{bmatrix} y_1(0) \\ y_1(1) \\ \vdots \\ y_1(M-1) \end{bmatrix} \tag{11}$$

In equations (8) and (9), first N_{cp} and M_{cp} rows are the CP's of y_0 and y_1, respectively.

$$\underbrace{\begin{bmatrix} y_0(0) \\ y_0(1) \\ \vdots \\ y_0(N_{cp}-1) \\ y_0(N_{cp}) \\ y_0(N_{cp}+1) \\ \vdots \\ y_0(N+N_{cp}-1) \end{bmatrix}}_{y_0} = \frac{1}{N} \begin{bmatrix} 1 & \bar{\omega}_0^{(N-N_{cp})} & \cdots & \bar{\omega}_0^{(N-1)(M-N_{cp})} \\ 1 & \bar{\omega}_0^{(N-N_{cp}+1)} & \cdots & \bar{\omega}_0^{(N-1)(M-N_{cp+1})} \\ \vdots & \vdots & \ddots & \vdots \\ 1 & \bar{\omega}_0^{(N-1)} & \cdots & \bar{\omega}_0^{(N-1)(N-1)} \\ 1 & 1 & \cdots & 1 \\ 1 & \bar{\omega}_0 & \cdots & \bar{\omega}_0^{(N-1)} \\ \vdots & \vdots & \ddots & \vdots \\ 1 & \bar{\omega}_0^{(N-1)} & \cdots & \bar{\omega}_0^{(N-1)(N-1)} \end{bmatrix} \begin{bmatrix} X_0(0) \\ X_0(1) \\ \vdots \\ X_0(N-1) \end{bmatrix} \tag{8}$$

Authorized licensed use limited to: Istanbul Medipol Universitesi. Downloaded on November 07,2022 at 06:26:24 UTC from IEEE Xplore. Restrictions apply.

$$\underbrace{\begin{bmatrix} y_1(0) \\ y_1(1) \\ \vdots \\ y_1(M_{cp}-1) \\ y_1(M_{cp}) \\ y_1(M_{cp}+1) \\ \vdots \\ y_1(M+M_{cp}-1) \end{bmatrix}}_{y_1} = \frac{1}{M} \begin{bmatrix} 1 & \bar{\omega}_1^{(M-M_{cp})} & \cdots & \bar{\omega}_1^{(M-1)(M-M_{cp})} \\ 1 & \bar{\omega}_1^{(M-M_{cp}+1)} & \cdots & \bar{\omega}_1^{(M-1)(M-M_{cp+1})} \\ \vdots & \vdots & \ddots & \vdots \\ 1 & \bar{\omega}_1^{(M-1)} & \cdots & \bar{\omega}_1^{(M-1)(M-1)} \\ 1 & 1 & \cdots & 1 \\ 1 & \bar{\omega}_1 & \cdots & \bar{\omega}_1^{(M-1)} \\ \vdots & \vdots & \ddots & \vdots \\ 1 & \bar{\omega}_1^{(M-1)} & \cdots & \bar{\omega}_1^{(M-1)(M-1)} \end{bmatrix} \begin{bmatrix} X_1(0) \\ X_1(1) \\ \vdots \\ X_1(M-1) \end{bmatrix} \tag{9}$$

Let us choose P subcarriers of numerology 0 and K subcarriers of numerology 1 at the neighbor boundary of both numerologies. That is, we take the last P subcarriers of numerology 0 from $\frac{N}{2}-P$ to $\frac{N}{2}-1$ subcarrier indexes, and the first K subcarriers of numerology 1 from $\frac{M}{2}$ to $\frac{M}{2}+K-1$ subcarrier indexes, from equations (2) and (3) to analyze and remove the INI on subcarriers to be transmitted.

A. *INI from numerology 0 to numerology 1-0 and 1-1*

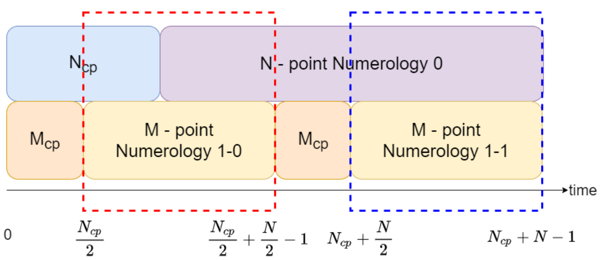

Fig. 1. INI from numerology 0 to numerology 1-0 and 1-1 in the time domain

The first part of numerology 0, shown in red dashed lines in Fig 1, between time samples $\frac{N_{cp}}{2}$ and $\frac{N_{cp}}{2}+\frac{N}{2}-1$ of subcarriers from $\frac{N}{2}-P$ to $\frac{N}{2}-1$ causes INI on subcarriers from $\frac{M}{2}$ to $\frac{M}{2}+K-1$ of numerology 1-0. This expression can be modeled as a matrix form in equation (12).

Eq. (12) can be simplified as in (13). Where, $\boldsymbol{INI}_{1,0}$ is a $K\times 1$-column vector that represents the INI on the first K subcarriers of numerology 1-0. $\boldsymbol{X}_0$ is the $P\times 1$-column vector of symbols to be transmitted of numerology 0 and $\boldsymbol{W}_{1,0}^{INI}$ is the $K\times P$ matrix describing how the INI is created.

$$\mathbf{INI}_{1,0} = \mathbf{W}_{1,0}^{INI}\mathbf{X}_0 \tag{13}$$

The second part of numerology 0, shown in blue dashed lines in Fig 1, between time samples $N_{cp}+\frac{N}{2}$ and $N_{cp}+N-1$ of subcarriers from $\frac{N}{2}-P$ to $\frac{N}{2}-1$ causes INI on subcarriers from $\frac{M}{2}$ to $\frac{M}{2}+K-1$ of numerology 1-1. This expression can be presented in a matrix form, as in equation (14), which also can be simplified as in (15).

$$\mathbf{INI}_{1,1} = \mathbf{W}_{1,1}^{INI}\mathbf{X}_0 \tag{15}$$

$$\underbrace{\begin{bmatrix} INI_{1,0(\frac{M}{2})} \\ INI_{1,0(\frac{M}{2}+1)} \\ \vdots \\ INI_{1,0(\frac{M}{2}+K-1)} \end{bmatrix}}_{\mathbf{INI}_{1,0}} = \underbrace{\begin{bmatrix} 1 & \cdots & \omega_1^{(\frac{M}{2})(M-1)} \\ 1 & \cdots & \omega_1^{(\frac{M}{2}+1)(M-1)} \\ \vdots & \ddots & \vdots \\ 1 & \cdots & \omega_1^{(\frac{M}{2}+K-1)(M-1)} \end{bmatrix} \frac{1}{N} \begin{bmatrix} \bar{\omega}_0^{(\frac{N}{2}-P)(\frac{N_{cp}}{2})} & \cdots & \bar{\omega}_0^{(\frac{N}{2}-2)(\frac{N_{cp}}{2})} & \bar{\omega}_0^{(\frac{N}{2}-1)(\frac{N_{cp}}{2})} \\ \vdots & \ddots & \vdots & \vdots \\ \bar{\omega}_0^{(\frac{N}{2}-P)(\frac{N_{cp}}{2}+\frac{N}{2}-1)} & \cdots & \bar{\omega}_0^{(\frac{N}{2}-2)(\frac{N_{cp}}{2}+\frac{N}{2}-1)} & \bar{\omega}_0^{(\frac{N}{2}-1)(\frac{N_{cp}}{2}+\frac{N}{2}-1)} \end{bmatrix}}_{\mathbf{W}_{1,0}^{INI}} \underbrace{\begin{bmatrix} X_0(\frac{N}{2}-P) \\ \vdots \\ X_0(\frac{N}{2}-2) \\ X_0(\frac{N}{2}-1) \end{bmatrix}}_{\mathbf{X}_0} \tag{12}$$

$$\underbrace{\begin{bmatrix} INI_{1,1(\frac{M}{2})} \\ INI_{1,1(\frac{M}{2}+1)} \\ \vdots \\ INI_{1,1(\frac{M}{2}+K-1)} \end{bmatrix}}_{\mathbf{INI}_{1,1}} = \underbrace{\begin{bmatrix} 1 & \cdots & \omega_1^{(\frac{M}{2})(M-1)} \\ 1 & \cdots & \omega_1^{(\frac{M}{2}+1)(M-1)} \\ \vdots & \ddots & \vdots \\ 1 & \cdots & \omega_1^{(\frac{M}{2}+K-1)(M-1)} \end{bmatrix} \frac{1}{N} \begin{bmatrix} \bar{\omega}_0^{(\frac{N}{2}-P)(N_{cp}+\frac{N}{2})} & \cdots & \bar{\omega}_0^{(\frac{N}{2}-2)(N_{cp}+\frac{N}{2})} & \bar{\omega}_0^{(\frac{N}{2}-1)(N_{cp}+\frac{N}{2})} \\ \vdots & \ddots & \vdots & \vdots \\ \bar{\omega}_0^{(\frac{N}{2}-P)(N_{cp}+N-1)} & \cdots & \bar{\omega}_0^{(\frac{N}{2}-2)(N_{cp}+N-1)} & \bar{\omega}_0^{(\frac{N}{2}-1)(N_{cp}+N-1)} \end{bmatrix}}_{\mathbf{W}_{1,1}^{INI}} \underbrace{\begin{bmatrix} X_0(\frac{N}{2}-P) \\ \vdots \\ X_0(\frac{N}{2}-2) \\ X_0(\frac{N}{2}-1) \end{bmatrix}}_{\mathbf{X}_0} \tag{14}$$

Authorized licensed use limited to: Istanbul Medipol Universitesi. Downloaded on November 07,2022 at 06:26:24 UTC from IEEE Xplore. Restrictions apply.

$$\underbrace{\begin{bmatrix} INI_{0,0(\frac{N}{2}-P)} \\ \vdots \\ INI_{0,0(\frac{N}{2}-2)} \\ INI_{0,0(\frac{N}{2}-1)} \end{bmatrix}}_{\mathbf{INI}_{0,0}} = \underbrace{\begin{bmatrix} 1 \cdots \omega_0^{(\frac{N}{2}-P)(\frac{N_{cp}}{2}+\frac{N}{2}-1)} \\ \vdots \ddots \quad \vdots \\ 1 \cdots \omega_0^{(\frac{N}{2}-2)(\frac{N_{cp}}{2}+\frac{N}{2}-1)} \\ 1 \cdots \omega_0^{(\frac{N}{2}-1)(\frac{N_{cp}}{2}+\frac{N}{2}-1))} \end{bmatrix} \frac{1}{M} \begin{bmatrix} \bar{\omega}_1^{(\frac{M}{2})(2M_{cp})} & \bar{\omega}_1^{(\frac{M}{2}+1)(2M_{cp})} & \cdots & \bar{\omega}_1^{(\frac{M}{2}+K-1)(2M_{cp})} \\ \bar{\omega}_1^{(\frac{M}{2})(2M_{cp}+1)} & \bar{\omega}_1^{(\frac{M}{2}+1)(2M_{cp}+1)} & \cdots & \bar{\omega}_1^{(\frac{M}{2}+K-1)(2M_{cp}+1)} \\ \vdots & \ddots & \vdots & \vdots \\ \bar{\omega}_1^{(\frac{M}{2})(M+M_{cp}-1)} & \bar{\omega}_1^{(\frac{M}{2}+1)(M+M_{cp}-1)} & \cdots & \bar{\omega}_1^{(\frac{M}{2}+K-1)(M+M_{cp}-1)} \end{bmatrix}}_{\mathbf{W}_{0,0}^{INI}} \underbrace{\begin{bmatrix} X_{1,0(\frac{M}{2})} \\ X_{1,0(\frac{M}{2}+1)} \\ \vdots \\ X_{1,0(\frac{M}{2}+K-1)} \end{bmatrix}}_{\mathbf{X}_{1,0}} \tag{16}$$

$$\underbrace{\begin{bmatrix} INI_{0,1(\frac{N}{2}-P)} \\ \vdots \\ INI_{0,1(\frac{N}{2}-2)} \\ INI_{0,1(\frac{N}{2}-1)} \end{bmatrix}}_{\mathbf{INI}_{0,1}} = \underbrace{\begin{bmatrix} \omega_0^{(\frac{N}{2}-P)(\frac{N}{2}+\frac{N_{cp}}{2})} & \cdots & \omega_0^{(\frac{N}{2}-P)(N-1)} \\ \vdots & \ddots & \vdots \\ \omega_0^{(\frac{N}{2}-2)(\frac{N}{2}+\frac{N_{cp}}{2})} & \cdots & \omega_0^{(\frac{N}{2}-2)(N-1)} \\ \omega_0^{(\frac{N}{2}-1)(\frac{N}{2}+\frac{N_{cp}}{2})} & \cdots & \omega_0^{(\frac{N}{2}-1)(N-1))} \end{bmatrix} \frac{1}{M} \begin{bmatrix} \bar{\omega}_1^{(\frac{M}{2})(M-M_{cp})} & \cdots & \bar{\omega}_1^{(\frac{M}{2}+K-1)(M-M_{cp})} \\ \vdots & \ddots & \vdots \\ 1 & \cdots & 1 \\ \vdots & \ddots & \vdots \\ \bar{\omega}_1^{(\frac{M}{2})(M-1)} & \cdots & \bar{\omega}_1^{(\frac{M}{2}+K-1)(M-1)} \end{bmatrix}}_{\mathbf{W}_{0,1}^{INI}} \underbrace{\begin{bmatrix} X_{1,1(\frac{M}{2})} \\ X_{1,1(\frac{M}{2}+1)} \\ \vdots \\ X_{1,1(\frac{M}{2}+K-1)} \end{bmatrix}}_{\mathbf{X}_{1,1}} \tag{18}$$

B. INI from numerology 1-0 and 1-1 to numerology 0

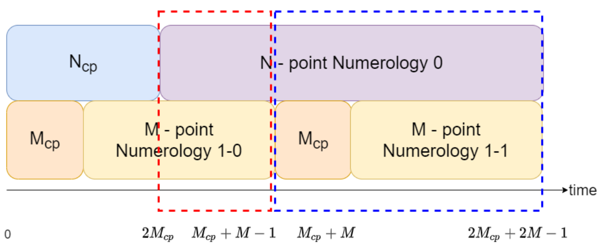

Fig. 2. INI from numerology 1-0 and 1-1 to numerology 0 in the time domain

Part of numerology 1-0, shown in red dashed lines in Fig. 2, between time samples $2M_{cp}$ and $M_{cp}+M-1$ of subcarriers from $\frac{M}{2}$ to $\frac{M}{2}+K-1$ causes INI on subcarriers from $\frac{N}{2}-P$ to $\frac{N}{2}-1$ of numerology 0. This expression can be modeled as a matrix form in equation (16), which can be simplified as

$$\mathbf{INI}_{0,0} = \mathbf{W}_{0,0}^{INI}\mathbf{X}_{1,0}, \tag{17}$$

where, $\boldsymbol{INI}_{0,0}$ is a $P \times 1$ column vector represents the INI created by numerology 1-0 on the last P subcarriers of numerology 0. $\boldsymbol{X}_{1,0}$ is the $K \times 1$ column vector of symbols to be transmitted of numerology 1-0 and $\boldsymbol{W}_{0,0}^{INI}$ is the $P \times K$ matrix describing how the INI is created.

The whole part of numerology 1-1, shown in blue dashed lines in Fig. 2, between time samples $M_{cp}+M$ and $2M_{cp}+2M-1$ of subcarriers from $\frac{M}{2}$ to $\frac{M}{2}+K-1$ causes INI on subcarriers from $\frac{N}{2}-P$ to $\frac{N}{2}-1$ of numerology 0. This expression can be modeled as a matrix form in equation (18), which can be simplified as

$$\mathbf{INI}_{0,1} = \mathbf{W}_{0,1}^{INI}\mathbf{X}_{1,1} \tag{19}$$

We should combine the equations (17) and (19) to get the whole INI on numerology 0.

$$\mathbf{INI}_0 = \mathbf{W}_{0,0}^{INI}\,\mathbf{X}_{1,0} + \mathbf{W}_{0,1}^{INI}\mathbf{X}_{1,1} \tag{20}$$

C. INI Modelling and INI Pre-Equalization Matrix

From equations (13), (15), (17), and (19), $K \times P$ matrices $\boldsymbol{W}_{1,0}^{INI}$, $\boldsymbol{W}_{1,1}^{INI}$ and $P \times K$ matrices $\boldsymbol{W}_{0,0}^{INI}$, $\boldsymbol{W}_{0,1}^{INI}$ are derived, respectively. By using equations (13), (15), and (20), the transmission symbols exposed to INI for each numerology can be written as

$$\begin{aligned} \mathbf{X}_0^{INI} &= \mathbf{X}_0 + \mathbf{W}_{0,0}^{INI}\mathbf{X}_{1,0} + \mathbf{W}_{0,1}^{INI}\mathbf{X}_{1,1} \\ \mathbf{X}_{1,0}^{INI} &= \mathbf{X}_{1,0} + \mathbf{W}_{1,0}^{INI}\mathbf{X}_0 \\ \mathbf{X}_{1,1}^{INI} &= \mathbf{X}_{1,1} + \mathbf{W}_{1,1}^{INI}\mathbf{X}_0 \end{aligned} \tag{21}$$

Equations in (21) can be shaped into a matrix form as

$$\begin{bmatrix} \mathbf{X}_0^{INI} \\ \mathbf{X}_{1,0}^{INI} \\ \mathbf{X}_{1,1}^{INI} \end{bmatrix} = \begin{bmatrix} \mathbf{I_P} & \mathbf{W}_{0,0}^{INI} & \mathbf{W}_{0,1}^{INI} \\ \mathbf{W}_{1,0}^{INI} & \mathbf{I_K} & \mathbf{0_K} \\ \mathbf{W}_{1,1}^{INI} & \mathbf{0_K} & \mathbf{I_K} \end{bmatrix} \begin{bmatrix} \mathbf{X}_0 \\ \mathbf{X}_{1,0} \\ \mathbf{X}_{1,1} \end{bmatrix} \tag{22}$$

where $\boldsymbol{I}_P$ and $\boldsymbol{I}_K$ denote $P \times P$ and $K \times K$ size identity matrices, respectively. $\boldsymbol{O}_K$ denotes the $K \times K$ size zero matrix. Therefore, equation (22) can be written as

$$\mathbf{X}^{INI} = \mathbf{W}^{INI}\mathbf{X} \tag{23}$$

where $\boldsymbol{X}^{INI}$ is a $(P+2K) \times 1$ column vector denotes transmission symbols exposed to INI. $\boldsymbol{W}^{INI}$ is the $(P+2K) \times (P+2K)$ matrix that models how INI is created at each numerologies' transmission symbols and $\boldsymbol{X}$ is the $(P+2K) \times 1$ column vector of transmission symbols that are exposed to INI. In other words, INI-free transmission symbols. Therefore, equation (23) models how transmission symbols are to be exposed to INI that occurs in the generation of the multi-numerology signals at the transmitter.

Authorized licensed use limited to: Istanbul Medipol Universitesi. Downloaded on November 07,2022 at 06:26:24 UTC from IEEE Xplore. Restrictions apply.

To remove INI on the transmission subcarriers (i.e symbols) completely, the transmission symbol vector, $\mathbf{X}$, should be pre-equalized. To do that, the inverse of $\boldsymbol{W}^{INI}$ should be used.

$$\mathbf{X}^b = (\mathbf{W}^{INI})^{-1}\mathbf{X} \tag{24}$$

Here, $(\mathbf{W}^{INI})^{-1}$ denotes the pre-equalization matrix, and $\boldsymbol{X}^b$ becomes a pre-equalized transmission symbol vector. In multi-numerology signal creation, using $\boldsymbol{X}^b$ instead of $\boldsymbol{X}$ will remove the INI on $\boldsymbol{X}$ as

$$\mathbf{X} = (\mathbf{W}^{INI})\mathbf{X}^b \tag{25}$$

Briefly, to eliminate INI on transmission symbols in multi-numerology creation, transmission symbols need to be pre-equalized by $(\mathbf{W}^{INI})^{-1}$. Note that, this is a fixed matrix and does not depend on instantaneously transmitted data. Therefore it is computed only once and used for all OFDM symbols.

In the simulations, the pre-equalization method is derived for numerology 0 (15 kHz) and numerology 1 (30 kHz). The 2 consecutive symbols of numerology 1, independent of each other, create an INI to numerology 0. Numerology 0 creates an INI to numerology 1-0 and numerology 1-1. These INI matrices can be formed into equation (22). In addition, this approach can be extended to other numerology pairs, such as numerology 0 (15 kHz) and numerology 2 (60 kHz). In this case, the 4 consecutive symbols of numerology 2, independent of each other, create an INI to numerology 0, and numerology 0 creates INI to numerology 2-0, 2-1, 2-2, and 2-3. In a similar way, the pre-equalization matrix in equation (22) could be derived.

Therefore, the INI pre-equalization method can be extended to all numerology pairs. The pre-equalization method eliminates all the INI that occured in those P and K values of subcarriers, and achieves theoretical BER performance.

IV. Numerical Results and Discussion

In this section, the performance of the proposed INI pre-equalization technique is evaluated in additive white Gaussian noise added to Rayleigh fading channels via Monte Carlo simulations. In the simulations, we consider $P = 96$ and $K = 48$ to give equal bandwidth for each numerology and only these bands will be considered for INI pre-equalization. Channel coding introduced in 5G and beyond is not considered throughout the simulations because the aim is to remove the INI that occurred on the transmission symbols. The total frequency bandwidth is divided equally for numerology 0 and 1. For this scenario, 256 and 128-point IDFT/DFT sizes are assigned to numerology 0 and 1, respectively. The guard band is not used between the numerologies and numerologies' CP lengths are chosen as 18 and 9, respectively. We consider 64-QAM and 256-QAM modulation levels for simulations.

First, generated multi-numerology OFDM signals via INI pre-equalization are directly demodulated without any noise and channel effect. After demodulation, it has been observed that the EVM values of the transmission symbols are 0 dB.

In Fig. 3 and 4, performances of INI pre-equalizer techniques are depicted by circle and triangle markers. Theoretical

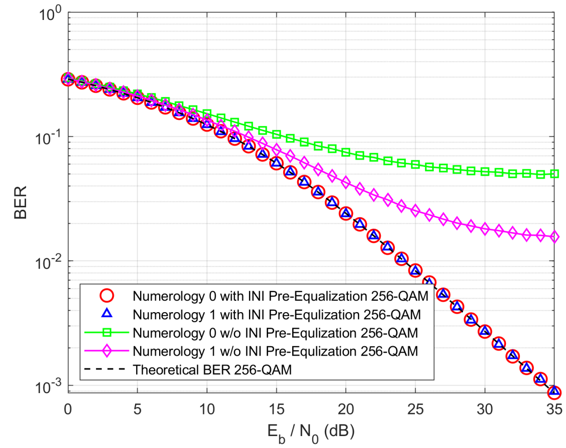

Fig. 3. BER results of 256-QAM for numerology 0 and 1

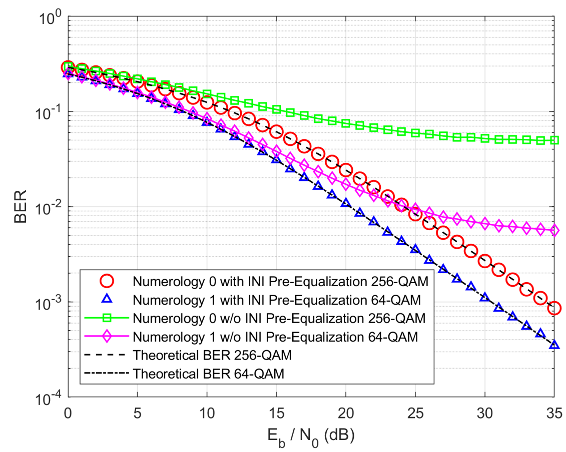

Fig. 4. BER results of 256-QAM and 64-QAM for numerology 0 and 1

BER performance (assuming no INI) is considered as the benchmark and the cases where the INI is not pre-equalized are shown with square and diamond markers. In Fig. 3 and 4, the BER performance of both numerologies is aligned with the theoretical BER in Rayleigh fading channel for both 64-QAM and 256-QAM.

We didn't compare our scheme with the guard-band-based schemes, since those methods result in a significant decrease in throughput. Besides, the performance of the pre-equalizer achieves the theoretical BER limits, which is already the best possible performance.

In Fig. 5, the PAPR analysis of INI pre-equalizer is investigated. Complementary cumulative distribution functions (CCDF) is taken into account. CCDF PAPR of pre-equalized multi-numerology signal is depicted by a circle and CCDF PAPR of non-pre-equalized multi-numerology signal is depicted by a triangle markers. The pre-equalization technique makes almost no changes to the PAPR while removing the INI.

Please note that only one $(\boldsymbol{W}^{INI})^{-1}$ square matrix of size $(P + 2K) \times (P + 2K)$ from (24) is used as a pre-equalizer to remove INI for any modulation scheme. This matrix only

Authorized licensed use limited to: Istanbul Medipol Universitesi. Downloaded on November 07,2022 at 06:26:24 UTC from IEEE Xplore. Restrictions apply.

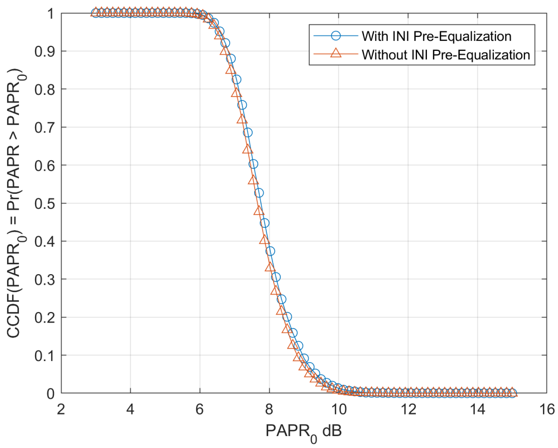

Fig. 5. PAPR CCDF results of 256-QAM for numerology 0 and 1

depends on the IDFT/DFT sizes, CP length, adjacent P and K subcarriers, and chosen numerology indices. After the pre-equalizer matrix is created once for a system, then the same matrix can be used for any modulations. Similar INI pre-equalizer matrices could be derived for other numerology pairs as $\mu = 0, 2$ and $\mu = 1, 2$ for any P and K values.

V. Conclusion

In this work, a pre-equalization solution for the removal of Inter numerology Interference (INI) in multi-numerology OFDM systems is proposed. The INI is mathematically expressed as a weighted linear combination of the transmitted symbols and the INI creation matrix is derived. Then, using an inverse of the INI creation matrix as a pre-equalizer we can completely remove the INI on the transmitter side for both numerologies. In future work, it is possible to further investigate to implement the proposed technique in multi-antenna systems and windowed-OFDM signals.

References

[1] T. T. Nguyen, V. N. Ha, and L. B. Le, "Wireless Scheduling for Heterogeneous Services With Mixed Numerology in 5G Wireless Networks," *IEEE Commun. Lett.*, vol. 24, no. 2, pp. 410–413, 2020.

[2] A. A. Zaidi, R. Baldemair, H. M. Tullberg, H. Bjorkegren, L. Sundström, J. Medbo, C. Kilinc, and I. L. D. Silva, "Waveform and Numerology to Support 5G Services and Requirements," *IEEE Commun. Mag.*, vol. 54, no. 11, pp. 90–98, 2016.

[3] A. Yazar and H. Arslan, "A Flexibility Metric and Optimization Methods for Mixed Numerologies in 5G and Beyond," *IEEE Access*, vol. 6, pp. 3755–3764, 2018. [Online]. Available: https://doi.org/10.1109/ACCESS.2018.2795752

[4] X. Cheng, R. Zayani, H. Shaiek, and D. Roviras, "Analysis and Cancellation of Mixed-Numerologies Interference for Massive MIMO-OFDM UL," *IEEE Wirel. Commun. Lett.*, vol. 9, no. 4, pp. 470–474, 2020.

[5] X. Zhang, L. Zhang, P. Xiao, D. Ma, J. Wei, and Y. Xin, "Mixed Numerologies Interference Analysis and Inter-Numerology Interference Cancellation for Windowed OFDM Systems," *IEEE Trans. Veh. Technol.*, vol. 67, no. 8, pp. 7047–7061, 2018.

[6] J. Mao, L. Zhang, P. Xiao, and K. Nikitopoulos, "Interference Analysis and Power Allocation in the Presence of Mixed Numerologies," *IEEE Trans. Wirel. Commun.*, vol. 19, no. 8, pp. 5188–5203, 2020.

[7] E. Memisoglu, A. B. Kihero, E. Basar, and H. Arslan, "Guard Band Reduction for 5G and Beyond Multiple Numerologies," *IEEE Commun. Lett.*, vol. 24, no. 3, pp. 644–647, 2020.

[8] S. Parkvall, E. Dahlman, A. Furuskar, and M. Frenne, "NR: The New 5G Radio Access Technology," *IEEE Commun. Stand. Mag.*, vol. 1, no. 4, pp. 24–30, 2017.

Authorized licensed use limited to: Istanbul Medipol Universitesi. Downloaded on November 07,2022 at 06:26:24 UTC from IEEE Xplore. Restrictions apply.